

Enhanced opportunistic beamforming scheme for practical broadcast systems[†]

R. Bosisio^{1*}, J. L. Vicario², U. Spagnolini¹ and C. Anton-Haro³

¹*Dipartimento Elettronica e Informazione, Politecnico di Milano, Piazza L. da Vinci 32, I-20133 Milano, Italy*

²*Departament de Telecomunicacions i Enginyeria de Sistemes, Universitat Autònoma de Barcelona, 08193 Bellaterra, (Cerdangola del Vallès), Spain*

³*Centre Tecnològic de Telecomunicacions de Catalunya, Av. Canal Olímpic S/N, 08860 Castelldefels, Barcelona, Spain*

SUMMARY

In multiantenna systems the optimisation of linear spatial precoding is severely hampered by the amount of feedback. A practical solution consists in the opportunistic beamforming (OB), which randomly generates the beamforming and schedules the user with the largest signal-to-noise ratio (SNR). In this paper we investigate the benefits that can be provided by the knowledge of the users spatial covariance at the transmitter. We enhance the OB scheme by matching the beamforming generation to the users channels spatial patterns. We analytically assess the performance of the proposed scheme, referred to as Cluster-Eigenbeamforming (Cluster-EB), both in ideal (perfect feedback) and in practical scenario (imperfect feedback). Cluster-EB is shown to outperform the conventional schemes and the performance gain increases in practical systems as Cluster-EB capitalises on the spatial covariance knowledge to reduce the sensitivity with respect to the feedback imperfections. Copyright © 2007 John Wiley & Sons, Ltd.

1. INTRODUCTION

Opportunistic beamforming (OB) [1, 2] has been recently proposed to exploit multiuser diversity (MUD) in broadcast wireless communication systems. OB is effective when an antenna array is employed at the base station (BS) and reduced feedback is mandatory as compared to other optimal strategies that require full channel state information (CSI) at the transmitter. The main idea is to generate a random beamforming at the BS and to schedule the users according to the signal-to-noise ratio (SNR) and some fairness requirements. A low-rate feedback channel is needed as the users have to report only the instantaneous SNR (I-CSI).

The OB scheme can be enhanced by capitalising on the knowledge at the BS of the channels spatial covariance, also known as long term CSI (LT-CSI) [3–5]. Since the channel spatial covariance can be assumed stationary over large time scale, it can be acquired by the transmitter either directly

from measurements on the opposite link or from limited feedback. The LT-CSI permits to match the beamforming generation to the spatial patterns of the users. To this aim, the eigenbeamforming (EB) technique [3] generates the beamforming vectors from the set of leading eigenvectors of the users' covariance matrices.

Following the approach in Reference [4], we say that users i and j are *spatially similar* when they have spatial covariance matrices \mathbf{R}_i and \mathbf{R}_j so that $\text{range}(\mathbf{R}_i) \simeq \text{range}(\mathbf{R}_j)$. The Cluster-Eigenbeamforming (Cluster-EB) scheme in Section 2 proposes to group the spatially similar users and to assign to each group one beamforming tailored on the spatial covariances of the clustered users. In each time slot the BS selects one cluster and transmits the corresponding beamforming. Then, the scheduler selects the user within the selected cluster that reports the largest SNR. We point out that the knowledge of the spatial covariance grants the spatial matching between the transmission beamforming

* Correspondence to: Roberto Bosisio, Dipartimento Elettronica e Informazione, Politecnico di Milano, Piazza L. da Vinci 32, I-20133 Milano, Italy. E-mail: rboisio@elet.polimi.it

[†]A Previous edition of this paper has been presented in the 12th European Wireless Conference (EW 2006), Athens, Greece.

and the users channel spatial patterns, whereas users clustering allows the scheduler to achieve MUD gain.

In Section 3 we analytically assess the performance of Cluster-EB in terms of scheduled SNR under the assumption of perfect I-CSI at the BS and we design the optimum beamforming configuration for each cluster. In Section 4 we focus on the sensitivity of the opportunistic schemes with respect to the imperfect knowledge of the multiuser feedback [5]. More specifically, we still assume that perfect LT-CSI as the estimation of the spatial covariance can be drawn over several training periods, but we deal with the imperfections in the I-CSI (instantaneous SNR) that may occur in practical systems. In Subsection 5.3 we investigate the impact of a practical (not ideal) SNR estimation technique at each mobile station (MS) by assuming that the estimator is based on a training sequence of N symbols. For small N the SNR estimation is strongly corrupted by errors, whereas the estimation accuracy improves when N increases. Then, in Subsection 5.4 we analyse the impact of a delay τ between the measurement at the MS and the downlink transmission of the scheduled users (i.e. in practical system the feedback outdated can be $\tau = 2$ ms as for HSDPA [6]). The delay makes the SNR employed at the scheduler to be an outdated version of the actual SNR, thus leading to a MUD degradation as pointed out in Reference [7]. Simulation results in Section 6 show that Cluster-EB outperforms OB and EB schemes and the performance benefits increase with the feedback degradation (small N or large τ). The reason is that users clustering based on spatial covariance exploits the reliability of the LT-CSI to increase the robustness against I-CSI degradation. Even in the limiting case of no I-CSI (i.e. $N = 0$ or $\tau \rightarrow \infty$), Cluster-EB grants the spatial matching between the scheduled user channel and the transmitted beam. The results confirm the efficiency of Cluster-EB and motivate its employment in practical systems, where reduced feedback is mandatory and I-CSI can be affected by imperfections. Finally, Section 7 draws some concluding remarks.

2. SYSTEM MODEL

Consider the downlink of system with a BS equipped with M antennas and n single-antenna mobile users. Let $\mathbf{x}(t)$ be the $M \times 1$ symbols vector transmitted at time t by the BS and let $y_i(t)$ be the signal at the i th receiver

$$y_i(t) = \sqrt{\alpha_i} \mathbf{h}_i^T(t) \mathbf{x}(t) + n_i(t) \quad (1)$$

where $\mathbf{h}_i(t) = [h_i^1(t) \cdots h_i^M(t)]^T$ is the complex channel vector, $n_i(t)$ the AWGN at the i th receiver with $n_i \sim CN(0, 1)$ and the scalar α_i denotes the average power of user i th.

Channel vector is zero-mean (Rayleigh fading) Gaussian distributed and it is modelled as $\mathbf{h}_i(t) = \mathbf{R}_i^{1/2} \mathbf{w}_i(t)$, where $\mathbf{w}_i(t) \sim CN(0, \mathbf{I}_M)$ and $\mathbf{R}_i = E[\mathbf{h}_i(t) \mathbf{h}_i^H(t)]$ is the $M \times M$ spatial covariance matrix for i th user with $\text{trace}(\mathbf{R}_i) = M$. We assume a time slot-based transmission and a block-fading model so that fading coefficients $\mathbf{w}_i(t)$ are constant within each time slot and vary independently across the time slots and the different users: $E[\mathbf{w}_i(t) \mathbf{w}_j(k)] = \delta(i - j) \delta(t - k)$. Covariance matrix \mathbf{R}_i is assumed constant over a large time scale and it is modelled according to the Lee's model [8], which assumes a ring of uniformly distributed scatters around the mobile terminals. In this scenario the correlation between the antenna elements reduces to

$$\mathbf{R}_i(p, q) = E[h_i^p(t) h_i^q(t)^*] = J_0(2\pi(p - q)\Delta) \cdot \psi_{i, \max} \cos(\phi_i) e^{-j2\pi(p - q)\Delta \sin(\phi_i)} \quad (2)$$

where $J_0(\cdot)$ is the Bessel function of the first kind of order zero, Δ is the antenna spacing in wavelength, ϕ_i is the angle of arrival relative to the i th user and $\psi_{i, \max}$ is the maximum angular spread.

At the beginning of each time slot the BS generates (see Section 3 for details on the different strategies) a beamforming vector $\mathbf{u}(t)$ with $\|\mathbf{u}(t)\|^2 = 1$, so that the transmitted signal $\mathbf{x}(t)$ can be expressed from the information symbols stream $s(t)$ as $\mathbf{x}(t) = \mathbf{u}(t)s(t)$. Each receiver (say i th) estimates the SNR

$$\gamma_i(t) = \alpha_i |\mathbf{h}_i^T(t) \mathbf{u}(t)|^2 \quad (3)$$

and sends back to the BS the corresponding estimation $\widehat{\gamma}_i(t)$. Optimal strategy with the aim of maximising the sum-rate is to select the user with the largest SNR. Nevertheless real systems are also concerned to guarantee fairness and latency requirements. In this paper we employ a simplified version of proportional fair (PF) algorithm [1, 9] that is based on the SNR instead of the achievable rate (as in conventional PF). The scheduler selects the user that maximises the ratio between the estimated SNR $\widehat{\gamma}_i(t)$ and the normalisation metric $T_i(t)$ drawn within a temporal window t_c . In other words, the PF scheduler selects in time slot t the user

$$i^* = \arg \max_i \widehat{\gamma}_i(t) / T_i(t) \quad (4)$$

where normalisation metric $T_i(t)$ is updated as

$$T_i(t + 1) = \begin{cases} (1 - 1/t_c)T_i(t) + \widehat{\gamma}_i(t)/t_c & \text{for } i = i^*, \\ (1 - 1/t_c)T_i(t) & \text{for } i \neq i^* \end{cases} \quad (5)$$

3. CLUSTER-EIGENBEAMFORMING (CLUSTER-EB)

3.1. Background

3.1.1. Conventional OB

The BS randomly generates the beamforming vector $\mathbf{u}(t)$ [1]. According to the propagation scenario described in Section 2, an efficient beam generation strategy consists in the phased array model

$$\mathbf{u}(t) = \frac{1}{\sqrt{M}} \left[1, e^{-j2\pi\Delta \sin \phi(t)}, \dots, e^{-j2\pi\Delta \sin \phi(t)(M-1)} \right]^T \quad (6)$$

where the angle $\phi(t)$ is randomly selected as $\phi(t) \sim U[-\pi/2, \pi/2]$ rad. Then, each user sends back to the BS the instantaneous SNR (3) and the scheduler prioritises the users with the best channel conditions according to the selection (4). This scheme is particularly effective for a large number n of users [2] and/or slowly varying fading channels as the beamforming fluctuation enhances the MUD gain [1].

3.1.2. Eigenbeamforming (EB)

Improvements over conventional OB can be obtained by assuming LT-CSI at the transmitter [3]. The EB strategy computes for each covariance \mathbf{R}_i for $i \in \{1, \dots, n\}$ the eigenvector \mathbf{v}_i corresponding to the largest eigenvalue

$\mathbf{v}_i = \max \text{eig}\{\mathbf{R}_i\}$. In each time slot t , the BS randomly selects the beamforming from the set of eigenvectors $\mathbf{u}(t) = \text{rand}\{\mathbf{v}_1, \dots, \mathbf{v}_n\}$, thus reducing the beams generation to the selection over a finite set. Still, each user feeds back the instantaneous SNR (3) and the BS schedules the largest normalised metric as in Equation (4). Of course, the user i th corresponding to the selected eigenvector (i.e. $\mathbf{u}(t) = \mathbf{v}_i$) is spatially matched. Anyway, we remark that the user scheduling policy (4) depends only on the reported SNR as a consequence of both the spatial matching and the instantaneous fading conditions.

3.2. Cluster-EB strategy

The Cluster-EB strategy is based on clustering the users into spatially similar characteristics according to the following steps [4]:

1. Group the n users into K clusters $\{\mathcal{C}_1, \dots, \mathcal{C}_K\}$ of high-correlated (spatially similar) elements by using the tree-based algorithm described in Subsection 3.3. As a result, each cluster \mathcal{C}_k for $k \in \{1, \dots, K\}$ contains n_k users so that $\sum_{k=1}^K n_k = n$.
2. For each cluster \mathcal{C}_k design a beamforming vector \mathbf{u}_k tailored on the spatial properties of the grouped users $i \in \mathcal{C}_k$ (see Section 4 for details).
3. In each time slot t select randomly one cluster as $k = \text{rand}\{1, \dots, K\}$ and transmit the beam $\mathbf{u}(t) = \mathbf{u}_k$.
4. The users $i \in \mathcal{C}_k$ send back their SNR and the scheduler selects the user belonging to \mathcal{C}_k that maximises the metric in Equation (4).

An intuitive insight on Cluster-EB is provided by Figure 1(a) under assumption that $\psi_{i,\max} = 0$ in Equation (2) (i.e. the covariance matrix depends only on the direction of arrival). Users located along similar directions

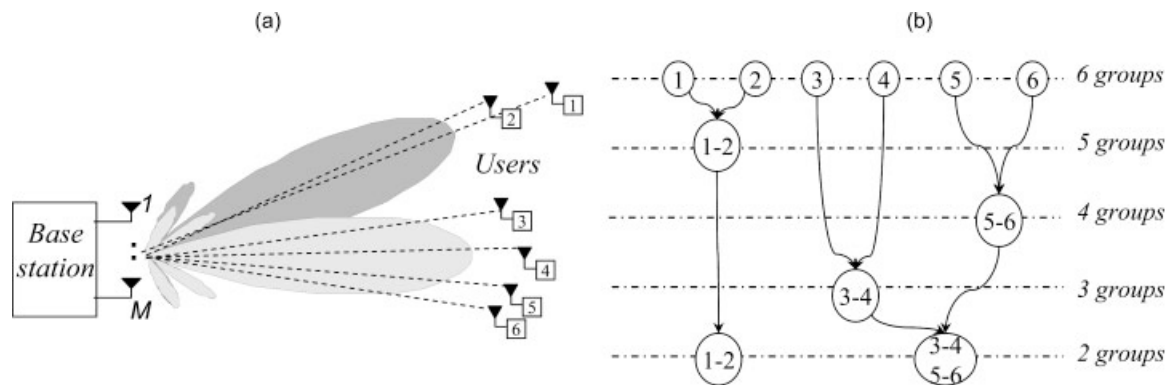


Figure 1. (a) Broadcast system with M antennas at the BS and $n = 6$ users. Users position here determines the correlation metric, (b) tree-based clustering for the $n = 6$ users in Subpart (a).

(1 and 2) have covariance matrices so that $\text{range}(\mathbf{R}_1) \simeq \text{range}(\mathbf{R}_2)$. The BS groups these users (1 and 2) and it transmits the corresponding spatial filtering (in figure the beamforming is focused on the middle to match both users' spatial patterns). Then, the scheduler achieves MUD gain by selecting the MS (1 or 2) that reports the largest SNR.

We notice that the strong correlation among the users sharing the same cluster guarantees the spatial matching between the transmitted beam \mathbf{u}_k and the users $i \in \mathcal{C}_k$ to be scheduled. At the same time, users clustering provides MUD as the opportunistic scheduler can select the user with the best channel conditions within the whole cluster. Thus, Cluster-EB provides a fair trade-off between the spatial matching (depending on the LT-CSI) and the MUD gain (that depends on the instantaneous fading conditions accounted by I-CSI). Finally, Cluster-EB permits to reduce the feedback rate as the BS requires feedback information to the subset of users belonging to the selected cluster.

3.3. Tree-based clustering algorithm

In this Section we review (see Reference [4] for more details) the framework for user clustering used in the Cluster-EB technique. Optimum grouping would be based on the range-spaces of each covariance matrix, thus requiring the modal decomposition $\mathbf{R}_i = \mathbf{U}_i \Lambda_i \mathbf{U}_i^H$, where matrices $\mathbf{U}_i = [\mathbf{u}_i^{(1)}, \dots, \mathbf{u}_i^{(M)}]$ and $\Lambda_i = \text{diag}(\lambda_i^{(1)}, \dots, \lambda_i^{(M)})$ contain the eigenvectors and the eigenvalues of \mathbf{R}_i , respectively. However, the corresponding computational complexity is unfeasible during scheduling process. To overcome this problem, we pursue here a low complexity clustering framework based on a scalar metric

$$\begin{aligned} \eta_{i,j} &= \frac{\text{tr}[\mathbf{R}_i \mathbf{R}_j^H]}{\sqrt{\text{tr}[\mathbf{R}_i \mathbf{R}_i^H] \text{tr}[\mathbf{R}_j \mathbf{R}_j^H]}} \\ &= \frac{\sum_{p,q} \lambda_i^{(p)} \lambda_j^{(q)} |\mathbf{u}_i^{(p)H} \mathbf{u}_j^{(q)}|^2}{\sqrt{\sum_p (\lambda_i^{(p)})^2 \sum_q (\lambda_j^{(q)})^2}} \end{aligned} \quad (7)$$

that provides a normalised measure of the average channel correlation. Equation (7) shows that the metric $\eta_{i,j}$ is an average of the square correlation of each pair of spatial modes $(\mathbf{u}_i^{(p)}, \mathbf{u}_j^{(q)})$ weighed by the corresponding modal $(\lambda_i^{(p)} \lambda_j^{(q)})$. Metric maximum ($\eta_{i,j} = 1$) is achieved when the users signal subspaces overlap completely (i.e. $\text{range}(\mathbf{R}_i) = \text{range}(\mathbf{R}_j)$), while minimum ($\eta_{i,j} = 0$) is obtained in case

of users channels spanning orthogonal subspaces (i.e. $\text{range}(\mathbf{R}_i) \perp \text{range}(\mathbf{R}_j)$).

For n users, we compute $n(n-1)/2$ metrics. Then, we perform a low-complexity tree-based approach that sequentially merges the users into groups of high-correlated elements as depicted in Figure 1(b). In the exemplary tree $n = 6$ users of Figure 1(a) are sequentially grouped in $K = 2$ clusters. At the first step, each user corresponds to a group. At each step we have one group less. This is achieved by merging two groups at the previous level into a single group. Between all the possible combinations, we select the pair (i, j) that maximises the metric $n_{i,j}$. The metric of the group obtained by merging is computed as $\eta_{(ij),z} = (\eta_{i,z} + \eta_{j,z})/2$ where $\eta_{(ij),z}$ is the metric between the group containing users i th and j th and a different user z th. Whenever the maximum of the metric $n_{i,j}$ between two group is lower than a given threshold η_{th} , the merging procedure is stopped.

4. PERFECT I-CSI

4.1. Normalisation metric

In this Section we investigate the asymptotic ($t \rightarrow \infty$) behaviour of the normalisation metric $T_i(t)$ in Equation (5) under assumption of perfect I-CSI at the BS (i.e. $\widehat{\gamma}_i(t) = \gamma_i(t)$). Notice that the normalisation metric $T_i(t)$ plays a key role in the overall performance evaluation as shown in Subsection 4.2. When t_c is large enough (i.e., $t_c \rightarrow \infty$), it can be proved [9] that the metric $T_i(t)$ weakly converges to the solution of the following equation

$$\frac{\partial T_i(t)}{\partial t} = T_i(t) - E[\gamma_i(t) | i = i^*] \Pr(i = i^*) \quad (8)$$

where $\Pr(i = i^*)$ stands for the probability that user i is scheduled. The expectation in Equation (8) is drawn over the ergodic instantaneous SNR, that is $\gamma_i(t) = \widehat{\gamma}_i(t)$. Random fluctuations are due to the channel and the beamforming variability. Equation (8) admits a steady state stationary solution $T_{i,\infty} = \lim_{t \rightarrow \infty} T_i(t)$ that can be obtained for each user $i \in \{1, \dots, n\}$ by solving the following set of n coupled Equations [9]

$$\begin{aligned} T_{i,\infty} &= E \left[\gamma_i \mid \frac{\gamma_i}{T_{i,\infty}} = \max \left(\frac{\gamma_1}{T_{1,\infty}}, \dots, \frac{\gamma_n}{T_{n,\infty}} \right) \right] \\ &\cdot \Pr \left(\frac{\gamma_i}{T_{i,\infty}} = \max \left(\frac{\gamma_1}{T_{1,\infty}}, \dots, \frac{\gamma_n}{T_{n,\infty}} \right) \right) \\ &\text{for } i = 1, \dots, n \end{aligned} \quad (9)$$

where we drop the index t in $\gamma_i(t)$ due to ergodicity assumption. Analytic derivation of $T_{i,\infty}$ in Equation (9) requires the knowledge of the probability density function (pdf) of the instantaneous SNR γ_i . This is far from being trivial for OB and EB techniques as the beamforming at the BS is time-varying.

However, in Cluster-EB the users belonging to cluster \mathcal{C}_k are always served when transmitting the beam \mathbf{u}_k so that the SNR γ_i of each users $i \in \mathcal{C}_k$ is distributed as χ_2^2 RV (for Rayleigh fading) with pdf $f_{\gamma_i}(\gamma_i) = 1/\bar{\gamma}_i e^{-\gamma_i/\bar{\gamma}_i}$ and average value $\bar{\gamma}_i = \alpha_i \mathbf{u}_k^H \mathbf{R}_i \mathbf{u}_k$. Since different clusters are served in different time slots, we can investigate the performance of each cluster separately. Without loss of generality, we focus on cluster \mathcal{C}_k and we assume $\mathcal{C}_k = \{1, \dots, n_k\}$. For each user i belonging to the k th cluster the normalisation metric converges to the solution of the same set of Equations (9)

$$T_{i,\infty} = \pi_k E \left[\gamma_i \middle| \frac{\gamma_i}{T_{i,\infty}} = \max \left(\frac{\gamma_1}{T_{1,\infty}}, \dots, \frac{\gamma_{n_k}}{T_{n_k,\infty}} \right) \right] \cdot \Pr \left(\frac{\gamma_i}{T_{i,\infty}} = \max \left(\frac{\gamma_1}{T_{1,\infty}}, \dots, \frac{\gamma_{n_k}}{T_{n_k,\infty}} \right) \right) \quad (10)$$

for $i = 1, \dots, n_k$

where π_k denotes the fraction of time allocated to the k th cluster. The expression above can be rearranged as

$$T_{i,\infty} = \pi_k \int_0^\infty \gamma_i f_{\gamma_i}(\gamma_i) \prod_{q=1, \dots, k, q \neq i} F_{\gamma_q} \left(\gamma_i \frac{T_{q,\infty}}{T_{i,\infty}} \right) d\gamma_i \quad (11)$$

for $i = 1, \dots, n_k$, where $F_{\gamma_i}(x) = \int_0^x f_{\gamma_i}(\gamma) d\gamma$ stands for the cumulative density function (cdf) of the instantaneous SNR γ_i . The set of equations in (11) admits a feasible solution for $T_{q,\infty}/T_{i,\infty} = \bar{\gamma}_q/\bar{\gamma}_i (\forall i, q \in \mathcal{C}_k)$. This allows to simplify $F_{\gamma_q}(\gamma_i T_{q,\infty}/T_{i,\infty}) = F_{\gamma_i}(\gamma_i)$ in Equation (11) and to decouple the expression of the steady state metric as

$$T_{i,\infty} = \pi_k \int_0^\infty \gamma_i f_{\gamma_i}(\gamma_i) F_{\gamma_i}(\gamma_i)^{n_k-1} d\gamma_i = \frac{\pi_k}{n_k} \bar{\gamma}_i \sum_{p=1}^{n_k} 1/p \quad (12)$$

where $\sum_{p=1}^{n_k} 1/p$ is the MUD gain for $n_k \chi_2^2$ RV (see [10]). The simplification in Equation (12) is due to the normalisation $\gamma_i/T_{i,\infty}$ in Equation (10), that makes the scheduler to operate over a set $\{\gamma_1/T_1, \dots, \gamma_{n_k}/T_{n_k}\}$ of independent and identically distributed χ_2^2 RVs regardless of the average channel conditions (i.e. $\bar{\gamma}_i$). The normalisation

makes the PF metric $T_{i,\infty}$ to be proportional to the average SNR $\bar{\gamma}_i$ and it guarantees a fair resource allocation (within each cluster \mathcal{C}_k) as an equal fraction of time is allocated to each user [9] (i.e. $\Pr(i = i^*) = \Pr(q = i^*)$).

Finally, in order to provide a fair resource allocation among the clusters, we select each cluster proportionally to the number of users (i.e. $\pi_k = \frac{n_k}{n}$) so that the asymptotic solution of the scheduling metric yields to

$$T_{i,\infty} = \frac{1}{n} \bar{\gamma}_i \sum_{p=1}^{n_k} 1/p \quad (13)$$

4.2. Performance analysis

The system performance is evaluated in terms of the aggregate average scheduled SNR $S = \sum_{i=1}^n S_i$, where

$$S_i = E[\gamma_i | i = i^*] \Pr(i = i^*) \quad (14)$$

is the average SNR for the scheduled user $E[\gamma_i | i = i^*]$ with the occurrence probability $\Pr(i = i^*)$. This will be referred to as average scheduled SNR. It can be easily seen that for perfect feedback and t_c large enough the average scheduled SNR S_i corresponds to the steady state normalisation metric $T_{i,\infty}$ (i.e. $T_{i,\infty} = S_i$). Then, by summing the scheduling metric in Equation (13) over the K clusters and over the users belonging to each cluster we obtain

$$S = \frac{1}{n} \sum_{k=1}^K \sum_{i \in \mathcal{C}_k} \bar{\gamma}_i \sum_{p=1}^{n_k} 1/p = \frac{1}{n} \sum_{k=1}^K \sum_{i \in \mathcal{C}_k} \alpha_i \mathbf{u}_k^H \mathbf{R}_i \mathbf{u}_k \sum_{p=1}^{n_k} 1/p \quad (15)$$

The expression (15) is maximised when the beam \mathbf{u}_k is the eigenvector relative to the largest eigenvalue of the matrix $\mathbf{R}_{\mathcal{C}_k} = [\alpha_1 \mathbf{R}_1, \dots, \alpha_{n_k} \mathbf{R}_{n_k}]$, which contains the users spatial subspaces scaled by users average power $\{\alpha_1, \dots, \alpha_{n_k}\}$.

We notice that the performance metric S is affected by two main components. The user SNR $\bar{\gamma}_i$ depends on the cluster geometrical properties, while the MUD gain $\sum_{p=1}^{n_k} 1/p$ is related on the number of users in each cluster. When each cluster consists in a single element ($n_k = 1$) the MUD vanishes. On the other hand, large clusters enhance the MUD gain and reduce the average users SNR $\bar{\gamma}_i$. Thus, system performance can be maximised by selecting a proper number of clusters in order to achieve a fair

trade-off between MUD and geometrical matching. In this paper we terminate the merging procedure of the tree-based algorithm (see Subsection 3.3) when the maximum metric $\eta_{i,j}$ between two groups is lower than the threshold value η_{th} . From our simulation we experienced that $\eta_{th} = 0.75$ is a reasonable trade-off.

5. IMPERFECT I-CSI

So far we have investigated the asymptotic properties that yield to the performance of the opportunistic scheduler when the BS is provided by perfect knowledge of the instantaneous SNR $\gamma_i(t)$. Anyway, in practical systems the I-CSI can be affected by degradations as it must be estimated at the MS and sent back to the BS via feedback channel. In Subsections 5.1 and 5.2 we analytically assess the sensitivity of the system performance in terms of average scheduled SNR S_i with respect to the I-CSI imperfections. In Subsection 5.3 we specialise the analysis by considering the employment of a data-aided SNR estimator at each MS. Next, in Subsection 5.4 we introduce a delay in the feedback channel so that the scheduler is provided by an outdated SNR.

5.1. Normalisation metric

In this section we assess the asymptotic behaviour of the normalisation metric $T_i(t)$ when $\hat{\gamma}_i(t) \neq \gamma_i(t)$ due to any imperfection in the I-CSI. For i th user belonging to cluster C_k , the asymptotic value of the metric $T_{i,\infty}$ at the BS can be expressed by the following set of equations

$$T_{i,\infty} = \pi_k E \left[\hat{\gamma}_i \left| \frac{\hat{\gamma}_i}{T_{i,\infty}} = \max \left(\frac{\hat{\gamma}_1}{T_{1,\infty}}, \dots, \frac{\hat{\gamma}_{n_k}}{T_{n_k,\infty}} \right) \right. \right] \cdot \Pr \left(\frac{\hat{\gamma}_i}{T_{i,\infty}} = \max \left(\frac{\hat{\gamma}_1}{T_{1,\infty}}, \dots, \frac{\hat{\gamma}_{n_k}}{T_{n_k,\infty}} \right) \right) \quad (16)$$

for $i = 1, \dots, n_k$

that can be rearranged as

$$T_{i,\infty} = \pi_k \int_0^\infty \hat{\gamma}_i g_{\hat{\gamma}_i}(\hat{\gamma}_i) \prod_{q=1, \dots, k, q \neq i} G_{\hat{\gamma}_q} \left(\hat{\gamma}_i \frac{T_{q,\infty}}{T_{i,\infty}} \right) d\hat{\gamma}_i \quad (17)$$

for $i = 1, \dots, n_k$, where $g_{\hat{\gamma}_i}(\hat{\gamma}_i)$ and $G_{\hat{\gamma}_i}(\hat{\gamma}_i)$ stands respectively for the pdf and the cdf of the estimated SNR $\hat{\gamma}_i$. We highlight the similarity between Equations (17) and (11). Thus, a feasible solution for Equation (17) is $T_{q,\infty}/T_{i,\infty} =$

$E[\hat{\gamma}_q]/E[\hat{\gamma}_i]$ so that the system of Equation (17) decouples as $T_{i,\infty} = \pi_k \int_0^\infty \hat{\gamma}_i g_{\hat{\gamma}_i}(\hat{\gamma}_i) G_{\hat{\gamma}_i}(\hat{\gamma}_i)^{n_k-1} d\hat{\gamma}_i$.

5.2. Performance analysis

The average scheduled SNR S_i in Equation (14) to be used for the performance analysis of the i th user belonging to cluster C_k can be expressed as

$$S_i = \pi_k E \left[\gamma_i \left| \frac{\hat{\gamma}_i}{T_{i,\infty}} = \max \left(\frac{\hat{\gamma}_1}{T_{1,\infty}}, \dots, \frac{\hat{\gamma}_{n_k}}{T_{n_k,\infty}} \right) \right. \right] \cdot \Pr \left(\frac{\hat{\gamma}_i}{T_{i,\infty}} = \max \left(\frac{\hat{\gamma}_1}{T_{1,\infty}}, \dots, \frac{\hat{\gamma}_{n_k}}{T_{n_k,\infty}} \right) \right) = \pi_k \int_0^\infty \gamma_i f_{\gamma_i}(\gamma_i | i = i^*) \Pr(i = i^*) d\gamma_i \quad (18)$$

for $i = 1, \dots, n_k$. The pdf of the scheduled SNR can be decomposed as

$$f_{\gamma_i}(\gamma_i | i = i^*) = \int_0^\infty f_{\gamma_i}(\gamma_i | \hat{\gamma}_i, i = i^*) g_{\hat{\gamma}_i}(\hat{\gamma}_i | i = i^*) d\hat{\gamma}_i = \int_0^\infty f_{\gamma_i}(\gamma_i | \hat{\gamma}_i) g_{\hat{\gamma}_i}(\hat{\gamma}_i | i = i^*) d\hat{\gamma}_i \quad (19)$$

where the second equality holds as the users undergo independent fading processes. By plugging Equation (19) into (18) we obtain

$$S_i = \pi_k \int_0^\infty \int_0^\infty \gamma_i f_{\gamma_i}(\gamma_i | \hat{\gamma}_i) g_{\hat{\gamma}_i}(\hat{\gamma}_i | i = i^*) \cdot \Pr(i = i^*) d\hat{\gamma}_i d\gamma_i, \quad \text{for } i = 1, \dots, n_k \quad (20)$$

When solving the expression above we notice that $g_{\hat{\gamma}_i}(\hat{\gamma}_i | i = i^*) \Pr(i = i^*) = g_{\hat{\gamma}_i}(\hat{\gamma}_i) \prod_{q \neq i} G_{\hat{\gamma}_q}(\hat{\gamma}_i \frac{T_{q,\infty}}{T_{i,\infty}}) = g_{\hat{\gamma}_i}(\hat{\gamma}_i) G_{\hat{\gamma}_i}(\hat{\gamma}_i)^{n_k-1}$ since it has been shown in Subsection 5.1 that $T_{q,\infty}/T_{i,\infty} = E[\hat{\gamma}_q]/E[\hat{\gamma}_i]$ so that it must be $G_{\hat{\gamma}_q}(\hat{\gamma}_i \frac{T_{q,\infty}}{T_{i,\infty}}) = G_{\hat{\gamma}_i}(\hat{\gamma}_i)$. It follows that the n_k equations in (20) decouple as

$$S_i = \pi_k \int_0^\infty \int_0^\infty \gamma_i f(\gamma_i | \hat{\gamma}_i) g_{\hat{\gamma}_i}(\hat{\gamma}_i) G_{\hat{\gamma}_i}(\hat{\gamma}_i)^{n_k-1} d\hat{\gamma}_i d\gamma_i \quad (21)$$

Now S_i can be evaluated as in Equation (21) for different impairments that make $\widehat{\gamma}_i(t) \neq \gamma_i(t)$ as shown below.

5.3. Estimated SNR

We will focus on user i th for the derivation of the SNR estimation algorithms. The received signal can be expressed from Equation (1) as $y_i(t) = r_i(t)s(t) + n_i(t)$, where $r_i(t) = \sqrt{\alpha_i} \mathbf{h}_i^T(t) \mathbf{u}_k$ is the equivalent scalar channel. We are interested in estimating the SNR $\widehat{\gamma}_i(t) = |r_i(t)|^2$ in each time slot t . In the sequel we drop the index t to ease the notation. Due to the block-fading assumption, we can perform intraslot SNR estimation using a ML estimator [11]

$$\widehat{\gamma}_i = \frac{|\mathbf{s}^H \mathbf{y}|^2}{N \mathbf{y}^H \mathbf{y} - |\mathbf{s}^H \mathbf{y}|^2} \quad (22)$$

where $\mathbf{s} = [s(0), \dots, s(N-1)]^T$ is the vector of transmitted pilot symbols and $\mathbf{y} = [y_i(0), \dots, y_i(N-1)]^T$ is the vector of received pilot symbols.

The pdf $f_{\gamma_i}(\gamma_i|\widehat{\gamma}_i)$ of the true SNR γ_i conditioned on the estimation $\widehat{\gamma}_i$ in Equation (22) and the pdf $g_{\widehat{\gamma}_i}(\widehat{\gamma}_i)$ of the estimated SNR $\widehat{\gamma}_i$ have been derived by using Bayes' rule in Reference [12] and are recalled in Appendix A. The derivation holds under assumption that γ_i is a χ_2^2 RV with average value $\bar{\gamma}_i$ as in case of Cluster-EB technique. By plugging $f_{\gamma_i}(\gamma_i|\widehat{\gamma}_i)$ and $g_{\widehat{\gamma}_i}(\widehat{\gamma}_i)$ into Equation (21) and after some algebra (see Appendix A for details) we obtain that the data-aided SNR estimation affects the system performance as follows

$$S_i = \frac{1}{n} \frac{1}{\bar{\gamma}_i + N} \cdot \left[1 + N^2 \bar{\gamma}_i \left(1 - n_k \frac{N-1}{N} \frac{\Gamma(n_k) \Gamma\left(1 + \frac{N}{N-1}\right)}{\Gamma\left(n_k + \frac{N}{N-1}\right)} \right) \right] \quad (23)$$

where $\Gamma(x) = \int_0^\infty t^{x-1} e^{-t} dt$ is the Gamma function defined in Reference [14].

In the limiting case of $n = 1$, it must be $K = n_k = 1$ and the expression (23) reduces to $S = S_1 = \bar{\gamma}_1$. In other words, the errors in the SNR estimation does not affect the scheduling performance as the system does not offer MUD. For any $n > 0$, when the number of pilots N increases, the estimation accuracy increases thus enhancing the system performance. By letting $N \rightarrow \infty$ the average scheduled SNR can be simplified (up to a negligible approximation for n_k large enough) to Equation (13) as $S_i \simeq \bar{\gamma}_i/n \sum_{p=1}^{n_k} 1/p$. On the other hand, in the limiting case of no I-CSI at the BS

(i.e. $N = 0$), the average scheduled SNR is $S_i \rightarrow \bar{\gamma}_i/n$ as in a conventional round robin (RR) scheme. We should remark that Cluster-EB always guarantees the spatial matching between the scheduled user i th belonging to cluster \mathcal{C}_k and the beam \mathbf{u}_k , thus leading to an high average SNR $\bar{\gamma}_i$ even when the I-CSI is strongly corrupted by noise (small N).

5.4. Outdated SNR

We here assume that the BS is provided by the outdated knowledge of the instantaneous SNR $\widehat{\gamma}_i(t) = |\mathbf{h}_i^T(t - \tau) \mathbf{u}_k|^2 = \gamma_i(t - \tau)$ for the channel $\mathbf{h}_i^T(t)$ and the beam \mathbf{u}_k when k th cluster is served. According to Jakes channel model, the channel $\mathbf{h}_i^T(t)$ is correlated with its delayed version $\mathbf{h}_i^T(t - \tau)$ by a correlation coefficient $\rho = J_0(2\pi f_D \tau)$ where f_D is the Doppler spread of the i th user. It follows that the conditional pdf of the instantaneous SNR γ_i conditioned to the delayed SNR $\widehat{\gamma}_i$ can be expressed as [13]

$$f_{\gamma_i}(\gamma_i|\widehat{\gamma}_i) = \frac{1}{(1 - \rho^2)\bar{\gamma}_i} \exp\left(-\frac{\rho^2 \widehat{\gamma}_i + \gamma_i}{(1 - \rho^2)\bar{\gamma}_i}\right) \cdot I_0\left(\frac{2\rho\sqrt{\widehat{\gamma}_i \gamma_i}}{(1 - \rho^2)\bar{\gamma}_i}\right) \quad (24)$$

for $\gamma, \widehat{\gamma} \geq 0$, where $I_0(\cdot)$ is the zero-order modified Bessel function of the first kind. On the other hand, the estimated SNR $\widehat{\gamma}_i$ is distributed as a scaled χ_2 RV with average value $\bar{\gamma}_i$. By plugging $f_{\gamma_i}(\gamma_i|\widehat{\gamma}_i)$ and $g_{\widehat{\gamma}_i}(\widehat{\gamma}_i)$ into Equation (21), the average scheduled SNR S_i yields to (see Appendix B for details)

$$S_i = \frac{\bar{\gamma}_i}{n} \left(\rho^2 \sum_{p=1}^{n_k} 1/p + (1 - \rho^2) \right) \quad (25)$$

We notice that the delay does not affect the performance when $n = 1$ as it must be $K = n_k = 1$ and expression (25) reduces to $S = S_1 = \bar{\gamma}_1$. In a more general case (i.e. $n > 1$), when the feedback channel is instantaneous ($\rho = 1$) Equation (25) leads to (13), while for completely decorrelated channel ($\rho = 0$) the scheduler can not exploit the MUD gain and the performance metric reduces to $S_i = \bar{\gamma}_i/n$ as in RR scheme. Thus, the MUD gain depends on the reliability of the I-CSI, while the spatial matching between scheduled user and beamforming is always guaranteed in Cluster-EB.

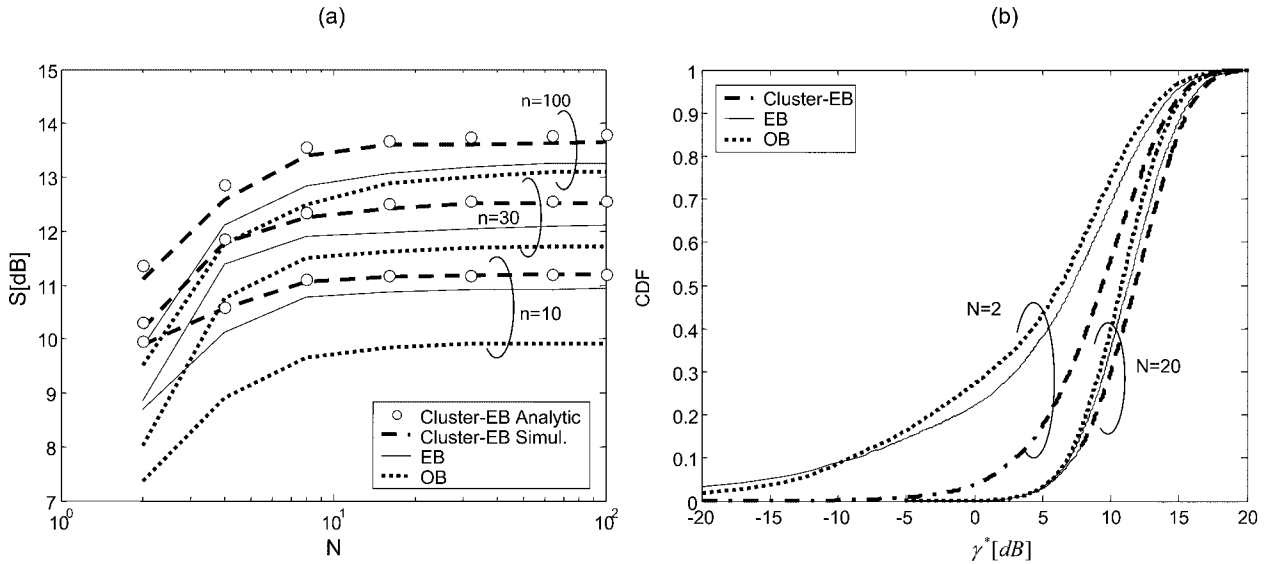


Figure 2. (a) Aggregate average scheduled SNR S versus pilot symbols N for Cluster-EB, EB and OB schemes. (b) Cumulative density function of the scheduled SNR γ^* . We consider $M = 6$ antennas at the BS, average power $10 \log_{10} \alpha_i \sim U[0, 5]$, angular spread $\psi_{i,\max} \sim U[0, 0.5]$ rad, $n = 10, 30, 100$ users in (a) and $n = 30$ users in (b).

6. NUMERICAL RESULTS

Here we investigate the performance of the opportunistic schemes with respect to the quality of the I-CSI at the transmitter. In our simulation scenario, the BS is equipped by $M = 6$ antennas, the maximum angular spread for each user i is $\psi_{i,\max} \sim U[0, 0.5]$ rad and the angle of departure is $\Phi_i \sim \mathcal{N}(\beta, 0.1)$ where β is drawn randomly from the set $[-\frac{\pi}{4}, 0, \frac{\pi}{6}, \frac{\pi}{3}]$ rad. Although the users are moving, we assume that the velocity is slow enough to make the angles and the spread (thus the spatial covariances) to be stationary over several time slots. The users power α_i is uniformly distributed (in dB) within the range $[0, 5]$ dB: $10 \log_{10} \alpha_i \sim U[0, 5]$. Proportional fairness scheduling is based on a temporal window of $t_c = 200$ time slots.

Figure 2(a) shows the average scheduled SNR $S = \sum_{i=1}^n S_i$ versus the number of pilot symbols N in a system with $n = 10, 30, 100$ active users. For $n = 10$ and $n = 30$ we obtain perfect matching between analytical evaluation (markers) of the Cluster-EB performance and the corresponding simulation results (dashed line). For $n = 100$ a little approximation is introduced by the assumption of large t_c (i.e. $t_c \rightarrow \infty$) as $t_c = 200$ is here comparable with the number of users n . Furthermore, we notice that, when using a large number of pilots N , the Cluster-EB performance saturates and asymptotically ($N \rightarrow \infty$) approaches the ideal feedback case (13). On the other hand, for limited training ($N = 2$) the I-CSI is strongly corrupted

by the estimation errors and the scheduler can not always select the user with the best channel condition. In this last case the performance of Cluster-EB reduces to that of the RR within each cluster and performance does not depend on the number of the users (no MUD gain).

We point out that Cluster-EB always outperforms EB and OB and the performance gap increases when increasing the I-CSI imperfection (small N). The reason is that Cluster-EB constrains the scheduler to select the MS among the set \mathcal{C}_k of users whose channels are spatially matched with the transmitted beam \mathbf{u}_k . Differently, the OB and EB scheduler selects the user out of the overall n users according to only the instantaneous information $\hat{\gamma}_i(t)$, that can be strongly corrupted by errors. The result is corroborated by Figure 2(b) which shows the cdf of the scheduled SNR $\gamma^*(t)$ defined as $\gamma^*(t) = \gamma_i(t)$ when $i = i^*$ in time slot t . It can be easily seen that $E[\gamma^*(t)] = S$. We consider $n = 30$ users in the cell and $N = 2, 20$ symbols in the training sequences. Cluster-EB offers effective performance (as compared to EB and OB) also for limited training ($N = 2$).

We have so far shown that the training sequence length N enhances the system performance as it allows the scheduler to prioritise the users with the best channel conditions and to achieve MUD gain. Anyway, the training sequence reduces the spectral efficiency due to the waste of transmission time. Let L be the number of symbols in each time slot, the transmission time reduces to $L - N$ due to transmission of N pilots. An upper bound on the transmission rate can be

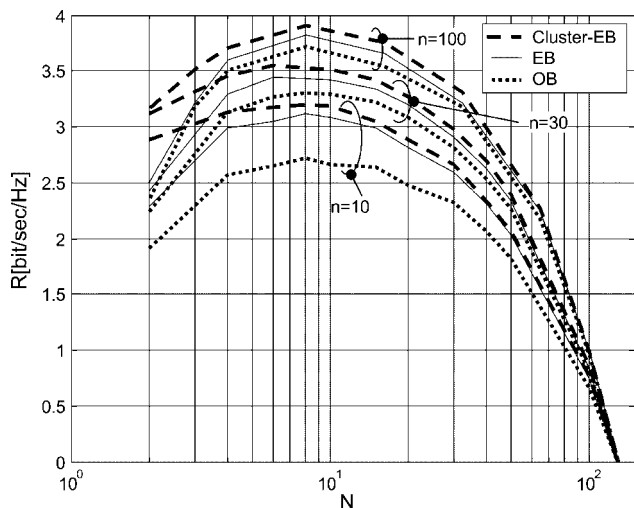


Figure 3. Spectral efficiency versus pilot symbols N for Cluster-EB, EB and OB schemes. We consider $M = 6$ antennas at the BS, average power $10 \log_{10} \alpha_i \sim U[0, 5]$, angular spread $\psi_{i,\max} \sim U[0, 0.5]$ rad and $n = 10, 30, 100$ users.

obtained by assuming that the maximum data rate granting reliable reception is $\log_2(1 + \gamma^*(t))$. It follows that the average spectral efficiency is $R = \frac{L-N}{L} E[\log_2(1 + \gamma^*(t))]$. It should be noted that here we are focusing on the impact of noisy SNR estimate on the scheduling process, whereas we neglect the impact of the channel estimation at the receiver and this motivates the use of the spectral efficiency (R) as an upper bound. This issue is out of the scope of

this work since we are interested in the analytical study of the scheduling impact. In Figure 3 we assess the trade-off between estimation accuracy and spectral efficiency for scenario with $n = 10, 30, 100$ users and $L = 128$ symbols per time slot. For small number of pilots the rate increases with N due to the increased estimation accuracy. For large N the rate decreases due to the transmission time reduction. The optimum number of pilots in this scenario is $N \simeq 10$, almost independent of the scheduling strategy.

In Figure 4(a) we investigate the aggregate average scheduled SNR S versus the channel decorrelation $\rho = J_0(2\pi f_D \tau)$ due to the delay τ between SNR estimation and scheduling when serving $n = 10, 100$ users. Solid lines depict the simulation results, whereas the markers stand for the analytical analysis (for Cluster-EB). For reduced feedback delay ($\rho \rightarrow 1$) the Cluster-EB increases with ρ till reaching (for $\rho = 1$) the ideal feedback performance (13). On the other hand, the scheduled SNR shows a floor in $S = 1/n \sum_{i=1}^n \bar{\gamma}_i$ for decorrelated channel ($\rho \rightarrow 0$) as the BS has no instantaneous information on the channel fading. In this last case the MUD gain vanishes and the performance of Cluster-EB reduces to that of a RR scheme within each cluster. Differently, in OB and EB the scheduled SNR still depends on n as the probability that the beam is spatially matched with the scheduled user increases with n (dense scenario). As in the estimated SNR case, Cluster-EB is less sensitive than OB and EB to the channel decorrelation as it always preserves the spatial matching between the transmitted beam \mathbf{u}_k and the physical channel. In other

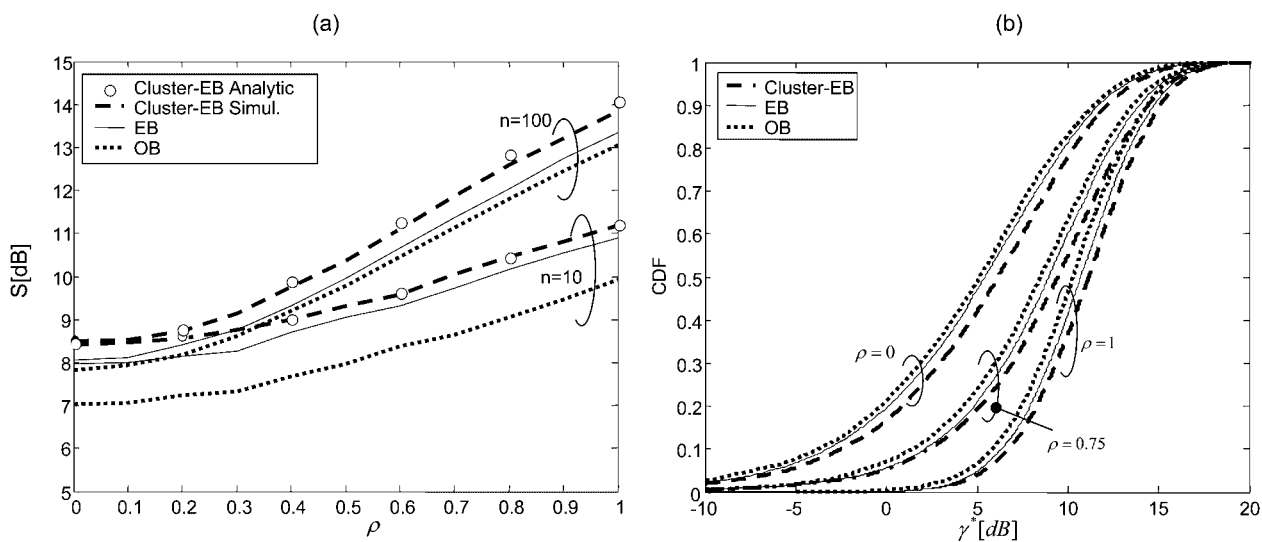


Figure 4. (a) Aggregate average scheduled SNR S versus channel decorrelation ρ for Cluster-EB, EB and OB schemes. (b) Cumulative density function of the scheduled SNR γ^* . We consider $M = 6$ antennas at the BS, average power $10 \log_{10} \alpha_i \sim U[0, 5]$, angular spread $\psi_{i,\max} \sim U[0, 0.5]$ rad, $n = 10, 100$ users in (a), $n = 30$ users and $\rho = 0, 0.75, 1$ in (b).

words, user clustering exploits the reliability of the LT-CSI to achieve robustness against the I-CSI imperfections. Finally, Figure 4(b) shows the cdf of the scheduled SNR for channel decorrelation $\rho = 0, 0.75, 1$ and $n = 30$ users.

7. CONCLUSIONS

In this paper it has been proposed an enhanced OB scheme based on the knowledge of the users spatial covariance at the BS. The main idea of the proposed Cluster-EB scheme is to group the spatially compatible users and to design an optimum beamforming for each group. Cluster-EB has been shown to provide a definite performance gain with respect to conventional opportunistic techniques. The advantages compared to the methods that make use of the spatial covariance improve when the knowledge of the instantaneous SNR is affected by imperfection due to not ideal SNR estimation or to the presence of a delay over the feedback channel. The moderate complexity of the proposed clustering algorithm and the robustness against imperfections make Cluster-EB well suited to a practical implementation.

APPENDIX A: PROOF OF EQUATION (23)

In Reference [12] the authors have derived the following distribution

$$f_{\gamma_i}(\gamma|\widehat{\gamma}) = \frac{1 + N\bar{\gamma}_i}{\bar{\gamma}_i} \left(\frac{1 + N\bar{\gamma}_i\widehat{\gamma}_i}{(1 + N\bar{\gamma}_i)(1 + \widehat{\gamma}_i)} \right)^N \cdot e^{-\gamma(N + \frac{1}{\bar{\gamma}_i})} {}_1F_1 \left(N, 1, \frac{N\bar{\gamma}_i\widehat{\gamma}_i}{1 + \widehat{\gamma}_i} \right) \quad (26)$$

$$g_{\widehat{\gamma}_i}(\widehat{\gamma}_i) = \frac{(N-1) \left(N + \frac{1}{\bar{\gamma}_i} \right)^{N-1}}{\bar{\gamma}_i \left((1 + \widehat{\gamma}_i) \left(N + \frac{1}{\bar{\gamma}_i} \right) - N\widehat{\gamma}_i \right)^N} \quad (27)$$

By recalling that $\pi_k = n_k/n$, by replacing Equation (26) into (21) and by switching the integration order we obtain

$$S_i = \frac{n_k}{n} \int_0^\infty \frac{\bar{\gamma}_i}{1 + N\bar{\gamma}_i} \left(1 + \frac{N^2\bar{\gamma}_i\widehat{\gamma}_i}{1 + N\bar{\gamma}_i + \widehat{\gamma}_i} \right) \cdot g_{\widehat{\gamma}_i}(\widehat{\gamma}_i) G_{\widehat{\gamma}_i}(\widehat{\gamma}_i)^{n_k-1} d\widehat{\gamma}_i \quad (28)$$

By plugging Equation (28) into (26) and by using the binomial expansion, the scheduled SNR can be resorted to (23).

APPENDIX B: PROOF OF EQUATION (25)

By substituting Equation (24) into (21) and by recalling that $\widehat{\gamma}_i$ is distributed as a χ_2 RV, we can express the average SNR scheduled to user i th as

$$S_i = \frac{n_k}{n} \int_{\gamma_i=0}^\infty \int_{\widehat{\gamma}_i=0}^\infty \frac{\gamma_i}{(1 - \rho^2)\bar{\gamma}_i^2} \exp \left(-\frac{\widehat{\gamma}_i + \gamma_i}{(1 - \rho^2)\bar{\gamma}_i} \right) \cdot I_0 \left(\frac{2\rho\sqrt{\widehat{\gamma}_i\gamma_i}}{(1 - \rho^2)\bar{\gamma}_i} \right) \left(1 - \exp \left(-\frac{\widehat{\gamma}_i}{\bar{\gamma}_i} \right) \right)^{n_k-1} d\widehat{\gamma}_i d\gamma_i \quad (29)$$

By using the binomial expansion and identities [14, Equation 6.614.3], [14, Equation 9.220.2] and [14, Equation 9.215.1], the following intermediate expression results

$$S_i = \frac{n_k}{n\bar{\gamma}_i} \sum_{z=0}^{n_k-1} \binom{n_k-1}{z} \frac{(-1)^z}{1 + z(1 - \rho^2)} \cdot \int_0^\infty \gamma_i \exp \left(-\frac{\gamma_i(z+1)}{\bar{\gamma}_i(1 + z(1 - \rho^2))} \right) d\gamma_i \quad (30)$$

Finally, by integrating by parts and after some manipulation one can easily achieve the result in expression (25).

ACKNOWLEDGMENT

This work was partially supported by Network of Excellence in Wireless Communications (NEWCOM) within Cluster 2.

REFERENCES

1. Viswanath P, Tse DNC, Laroia R. Opportunistic beamforming using dumb antennas. *IEEE Transactions on Information Theory* 2002; **48**(6):1277–1294.
2. Sharif M, Hassibi B. On the capacity of MIMO broadcast channels with partial side information. *IEEE Transactions on Information Theory* 2005; **51**(2):506–522.
3. Senst A, Schulz-Rittich P, Krause U. Random beamforming in correlated MISO channels for multiuser systems. In *IEEE International Conference on Communications* Vol. 5, 2004; pp. 2909–2913.
4. Bosisio R, Spagnolini U. Users clustering based on covariance feedback in broadcast opportunistic beamforming schemes. *Proceedings of IEEE WSA 2006*.
5. Bosisio R, Vicario JL, Anton C, Spagnolini U. The effect of imperfect feedback on broadcast opportunistic schemes. *Proceedings of European Wireless 2006*.

6. Holma H, Toskala A (eds). *WCDMA for UMTS, Radio Access for Third Generation Mobile Communications*. Wiley.
7. Kobayashi M, Caire G, Gesbert D. Transmit diversity vs. opportunistic beamforming in packet data downlink transmission. *IEEE Transactions on Wireless Communications* 2005 (in press).
8. Fulghum T, Molnar K. The Jakes fading model incorporating angular spread for a disk of scatterers. *Proceedings of IEEE VTC 1998 May 1998*; pp. 489–493.
9. Kushner HJ, Whiting PA. Convergence of proportional-fair sharing algorithms under general conditions. *IEEE Transactions on Wireless Communications* 2004; **3**:1250–1259.
10. David HA, Nagaraja HN. *Order Statistics*, 3rd edn. Wiley, 2003.
11. Pauluzzi DR, Beaulieu NC. A comparison of SNR estimation techniques for the AWGN channel. *IEEE Transactions on Communications* 2000; **48**:1681–1691.
12. Schulz-Rittich P, Senst A, Bilke T, Meyr H. The effect of imperfect SNR knowledge on multiantenna multiuser systems with channel aware scheduling. *Proceedings of IEEE GLOBECOM 2003*, Vol. 1, 2003; pp. 153–157.
13. Simon MK, Alouini M-S. *Digital Communications over Fading Channels: A Unified Approach to Performance Analysis*. Wiley, 2000.
14. Gradshteyn IS, Ryzhik IM. *Tables of Integrals; Series and Products*. Academic: New York, 1965.